

Slow waves in fractures filled with viscous fluid

Valeri Korneev¹

ABSTRACT

Stoneley guided waves in a fluid-filled fracture generally have larger amplitudes than other waves; therefore, their properties need to be incorporated into more realistic models. A fracture is modeled as an infinite layer of viscous fluid bounded by two elastic half-spaces with identical parameters. For small fracture thickness, a simple dispersion equation for wave-propagation velocity is obtained. This velocity is much smaller than the velocity of a fluid wave in a Biot-type solution, in which fracture walls are assumed to be rigid. At seismic prospecting frequencies and realistic fracture thicknesses, the Stoneley guided wave has wavelengths on the order of several meters and a quality factor Q exceeding 10, which indicates the possibility of resonance excitation in fluid-bearing rocks. The velocity and attenuation of Stoneley guided waves are distinctly different at low frequencies for water and for oil. The predominant role of fractures in fluid flow at field scales is supported by permeability data, showing an increase of several orders of magnitude when compared with values obtained at laboratory scales. The data suggest that Stoneley guided waves should be taken into account in theories describing seismic wave propagation in fluid-saturated rocks.

INTRODUCTION

Stoneley guided waves in fractures are described by Ferrazzini and Aki (1987), who use them to explain low-frequency tremors observed before volcanic eruptions. Earlier, Chouet (1986) suggested that such tremors are caused by resonances in molten lava during fracture opening. Because of the large (0.5–1.0 m) fracture thickness in those earlier investigations, the fluid viscosity was not considered. Such a slow fluid wave is a Stoneley wave, one that propagates in a waveguide formed by a fluid layer bounded by elastic walls. Krauklis (1962) describes such a wave, but no application is mentioned. Ferrazzini and Aki (1987) rederive the slow Stoneley

wave as a fundamental symmetrical mode that propagates along the fracture with a velocity that approaches zero at low frequency. They stop short of deriving the low-frequency asymptote for a phase velocity of this wave (see their equation 16), which can be obtained in the form

$$V_{f0} = \left(\frac{\omega h \mu}{\rho_f} (1 - \gamma^2) \right)^{\frac{1}{3}}, \quad (1)$$

where frequency is ω , fracture thickness is h , fluid density is ρ_f , shear modulus of the elastic walls is μ , and elastic velocities ratio is $\gamma = V_s/V_p$.

Fluid-filled fracture waves have been studied numerically and in the laboratory (Paillet and White, 1982; Groenenboom and Fokkema, 1998; Groenenboom and Falk, 2000; Groenenboom and van Dam, 2000) for monitoring hydrofracture processes, including the effect of diffraction at the tip of the fracture. Those studies confirm the existence of a slow fluid wave in such models and demonstrate its predominantly high amplitude (Groenenboom and Fokkema, 1998). The dispersive wave represented by equation 1 has a variety of names (e.g., slow fluid wave, fluid guided wave, Stoneley guided wave, first symmetrical fluid mode), all of which have the same meaning.

Molotkov and Bakulin (1998) show that for infinite fracture models, a stack of fractures filled with nonviscous fluid has a solution in the form of the second Biot wave propagating in a transversely isotropic medium with frequency-independent velocity. Goloshubin et al. (1994) find that the slow Stoneley wave also can propagate in such a medium when it is sandwiched between two elastic half-spaces. An unbounded stack of fractures containing viscous fluid is capable of carrying frequency-dependent, slow Biot waves (Schoenberg, 1983, 1984; Gurevich, 2002). It is yet unclear if such a model also could carry a Stoneley wave, which has a lower velocity.

Slow fluid waves are essential for generating tube-wave reflections from intersecting fractures (Hornby et al., 1989; Kostek et al., 1998a, b). The high amplitudes of such waves make solving relevant problems rather simple because we can ignore most other types of waves without compromising the result. Comparisons with exact solutions (Kostek et al., 1998a) show that considering only fluid waves

Manuscript received by the Editor 23 February 2007; revised manuscript received 30 July 2007; published online 9 November 2007.

¹Lawrence Berkeley National Laboratory, Earth Sciences Division, Berkeley, California. E-mail: vakorneev@lbl.gov.

© 2008 Society of Exploration Geophysicists. All rights reserved.

in seemingly difficult problems is well justified. The energy-trapping ability of such waves illustrates the distinctive feature of fluid-filled fractures — specifically, their waveguidelike capability of transporting energy (similar to electric current transported by metal wires). Hornby et al. (1989) and Kostek et al. (1998a) also show that the reflection amplitude of tube waves from a fracture is frequency dependent and increases as the frequency approaches zero.

Strong evidence exists that an adequate theory of seismic wave propagation in fluid-saturated rock requires incorporating fracture fluid waves. From hydrogeology results, it follows that some scaling rules need to be applied to laboratory permeability measurements before using them at field scale. In hydrologic experiments, the permeability parameter can be evaluated at the laboratory scale (0.01–0.1 m) by measuring fluid-flow rate through a rock sample in the presence of a fluid-pressure gradient. At the 10–100-m field scale, permeability is evaluated routinely by using well tests (Muskat, 1946); at a 100–1000-m scale, permeability generally is determined by using tracer tests. Therefore, laboratory and field scales can differ by about five orders of magnitude.

Measurements of permeability (hydraulic conductivity) for a wide range of scales have been done in comprehensive studies for a variety of geologic environments (Clauser, 1992; Gelhar, 1993; Neuman, 1994; Schulze-Makuch and Cherkauer, 1998; Schulze-Makuch et al., 1999). Typically, an increase of five orders of scale corresponds to five to seven orders of permeability increase. Such scaling behavior suggests the dominant role of fractures in fluid flow at field scales. Biot-Gassmann poroelasticity theory (Gassmann, 1951; Biot, 1956a, b; 1962) treats fluids in fractures as flowing between rigid walls. It does not describe the existence of slow fluid waves that require elastic walls. However, the importance of slow fluid waves for seismic wave propagation in fluid-bearing rock needs justification.

Rock fluids, such as water or oil, have some natural viscosity that causes attenuation of propagating fluid waves. At the same time, the thicknesses of real fractures might be on the order of millimeters or less. Can slow fluid waves propagate and cause resonances in real fractures? To answer this question, we need to evaluate for realistic parameters the attenuation of slow fluid waves caused by fluid viscosity, which is the subject of this paper.

THEORY

Stoneley slow wave

Consider a symmetrical model of a layer $-h/2 \leq z \leq h/2$, filled with viscous fluid between two homogeneous elastic half-spaces (Figure 1) with the same material parameters. Here, derivations similar to those from Ferrazzini and Aki (1987) are used. In the following, index $j = 1$ indicates the parameters and fields related to the layer; index $j = 2$ indicates the values related to half-spaces. As also shown in Figure 1, we consider propagation of symmetrical wave modes along the OX axis of the x spatial coordinate.

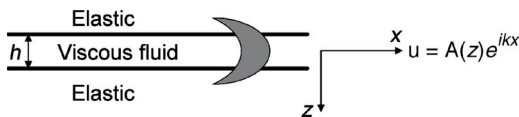


Figure 1. A layer filled with viscous fluid between two elastic half-spaces.

In a medium with nonzero shear modulus, two body waves can propagate: a longitudinal (P) wave with velocity

$$V_{Pj} = \sqrt{\frac{\lambda_j + 2\mu_j}{\rho_j}} \quad (2)$$

and a shear (S) wave with velocity

$$V_{Sj} = \sqrt{\frac{\mu_j}{\rho_j}}, \quad (3)$$

expressed through Lamé constants λ_j and μ_j and through density ρ_j , where ($j = 1, 2$).

Combining a linearized equation for compressible viscous fluid (Landau and Lifshitz, 1959) with a continuity relation, the equation for viscous fluid velocity motion can be obtained in the form

$$\begin{aligned} \frac{\partial^2 \mathbf{u}}{\partial t^2} - \frac{\eta}{\rho_f} \nabla^2 \frac{\partial \mathbf{u}}{\partial t} - \frac{1}{\rho_f} \left(\xi - \frac{\eta}{3} \right) \nabla \nabla \cdot \frac{\partial \mathbf{u}}{\partial t} - c_p^2 \nabla \nabla \cdot \mathbf{u} \\ = 0, \end{aligned} \quad (4)$$

with time t , fluid density $\rho_f = \rho_1$, and viscosity coefficients η and ξ ; the speed of sound in the absence of viscosity is c_p . Particle velocity \mathbf{u} in equation 4 can be represented as the sum

$$\mathbf{u} = \mathbf{u}_p^{(1)} + \mathbf{u}_s^{(1)}, \quad (5)$$

where $\mathbf{u}_p^{(1)}$ and $\mathbf{u}_s^{(1)}$ are compressional and shear components, respectively. These components obey the equations

$$\nabla \times \mathbf{u}_p^{(1)} = 0, \quad \nabla \cdot \mathbf{u}_s^{(1)} = 0 \quad (6)$$

and satisfy equations of motion

$$\frac{\partial^2 \mathbf{u}_p^{(1)}}{\partial t^2} - \frac{1}{\rho_f} \left(\xi + \frac{4\eta}{3} \right) \nabla \nabla \cdot \frac{\partial \mathbf{u}_p^{(1)}}{\partial t} - c_p^2 \nabla \nabla \cdot \mathbf{u}_p^{(1)} = 0 \quad (7)$$

and

$$\frac{\partial^2 \mathbf{u}_s^{(1)}}{\partial t^2} + \frac{\eta}{\rho_f} \nabla \times \nabla \times \frac{\partial \mathbf{u}_s^{(1)}}{\partial t} = 0. \quad (8)$$

Using the time dependence of the fields in the form $\exp(-i\omega t)$, with angular frequency ω , equations 7 and 8 correspondingly describe the propagation of dissipating P- and S-waves with complex velocities:

$$V_{P1} = \sqrt{c_p^2 - i \frac{\omega}{\rho_f} \left(\xi + \frac{4\eta}{3} \right)}, \quad (9)$$

$$V_{S1} = \sqrt{-\frac{i\omega\eta}{\rho_f}}, \quad (10)$$

and complex Lamé constants:

$$\lambda_1 = c_p^2 \rho_f - i\omega \left(\xi - \frac{2\eta}{3} \right), \quad (11)$$

$$\mu_1 = -i\omega\eta. \quad (12)$$

Shear waves in fluid appear exclusively because of viscosity and have diffusive propagation types. Displacements $\mathbf{u}_p^{(j)}$ and $\mathbf{u}_s^{(j)}$, ($j = 1, 2$), relate to potentials φ_j and ψ_j through the following equations:

$$\mathbf{u}_p^{(j)} = \nabla \varphi_j, \quad (13)$$

$$\mathbf{u}_s^{(j)} = \nabla \times (\psi_j \mathbf{y}_1), \quad (14)$$

where the unit vector \mathbf{y}_1 is used. We seek a solution in the form of a surface wave with wavenumber $k_x = \omega/V_f$, propagating along the OX axis with phase velocity V_f . For the symmetrical mode, the potentials have the forms

$$\varphi_1 = A_1 \left(e^{k_x \sqrt{1 - \alpha_{p1}^2} z} + e^{-k_x \sqrt{1 - \alpha_{p1}^2} z} \right) e^{ik_x x}, \quad (15)$$

$$\psi_1 = B_1 \left(e^{k_x \sqrt{1 - \alpha_{s1}^2} z} - e^{-k_x \sqrt{1 - \alpha_{s1}^2} z} \right) e^{ik_x x} \quad (16)$$

inside the layer and

$$\varphi_2 = A_2 e^{-k_x \operatorname{sign}(z) \sqrt{1 - \alpha_{p2}^2} z} e^{ik_x x}, \quad (17)$$

$$\psi_2 = B_2 e^{-k_x \operatorname{sign}(z) \sqrt{1 - \alpha_{s2}^2} z} e^{ik_x x} \quad (18)$$

outside the layer, where

$$\alpha_{pj} = \frac{\omega}{k_x V_{pj}} = \frac{V_f}{V_{pj}}, \quad \alpha_{sj} = \frac{\omega}{k_x V_{sj}} = \frac{V_f}{V_{sj}}, \quad (j = 1, 2), \quad (19)$$

and A_j and B_j are constants determined from the boundary conditions.

Boundary conditions at interfaces $z = \pm h/2$ require continuity of displacements and stress, which have the components

$$\tau_{xz}^{(j)} = 2\mu_j \frac{\partial^2 \varphi_j}{\partial x \partial z} + \mu_j \left(\frac{\partial^2 \psi_j}{\partial x^2} - \frac{\partial^2 \psi_j}{\partial z^2} \right), \quad (20)$$

$$\tau_{zz}^{(j)} = \lambda_j \nabla^2 \varphi_j + 2\mu_j \left(\frac{\partial^2 \psi_j}{\partial z^2} - \frac{\partial^2 \psi_j}{\partial x \partial z} \right), \quad (21)$$

$$(j = 1, 2).$$

Because symmetry is embedded in the solution, we need to satisfy boundary conditions on just one interface. The problem has four unknowns, A_j, B_j ($j = 1, 2$), with four equations at the boundary using two components for both stress and displacement. The dispersion equation for symmetrical modes is obtained by finding values of V_f for which the determinant of the system is zero. Using $z = h/2$, we can obtain (after some algebra) the equation

$$\begin{aligned} & (1 - c)^2 \xi_1 \xi_2 \chi_1 \chi_2 - (b - c)^2 \xi_1 \chi_1 - c(1 - a)(1 - b) \\ & \times [\xi_2 \chi_1 + \xi_1 \chi_2] - (1 - ac)^2 \xi_2 \chi_2 + (ca - b)^2 \\ & = 0, \end{aligned} \quad (22)$$

where

$$\xi_1 = \sqrt{1 - \alpha_{p1}^2} \tanh \left(\sqrt{1 - \alpha_{p1}^2} \frac{k_x h}{2} \right), \quad (23)$$

$$\chi_1 = \sqrt{1 - \alpha_{s1}^2} \coth \left(\sqrt{1 - \alpha_{s1}^2} \frac{k_x h}{2} \right), \quad (24)$$

$$\xi_2 = \sqrt{1 - \alpha_{p2}^2}, \quad (25)$$

$$\chi_2 = \sqrt{1 - \alpha_{s2}^2}, \quad (26)$$

and coefficients a , b , and c have expressions

$$a = 1 - \frac{\alpha_{s1}^2}{2}, \quad b = 1 - \frac{\alpha_{s2}^2}{2}, \quad c = \frac{\mu_1}{\mu_2}. \quad (27)$$

The roots of equation 22 provide all possible symmetrical modes for the problem. However, only the low-frequency mode corresponding to the slow fluid wave is considered hereafter. Assuming that both frequency ω and thickness h are small enough, the argument in equation 23 is

$$\left| \sqrt{1 - \alpha_{p1}^2} \frac{k_x h}{2} \right| \ll 1. \quad (28)$$

In addition, if the velocity V_f is small enough,

$$|\alpha_{p1}| \ll 1, \quad |\alpha_{p2}| \ll 1 \quad \text{and} \quad |\alpha_{s2}| \ll 1, \quad (29)$$

then equation 22 yields

$$\chi_1 \left[k_x h - \frac{\rho_f \alpha_{s2}^2}{\rho_2 (1 - \gamma^2)} \right] = 2. \quad (30)$$

We also assume that phase velocity V_f is much larger than shear-wave velocity V_{s1} in the viscous fluid, providing the condition

$$|\alpha_{s1}| \gg 1. \quad (31)$$

For thin fractures, when

$$\left| \sqrt{1 - \alpha_{s1}^2} \frac{k_x h}{2} \right| \approx \frac{S}{2} \ll 1, \quad (32)$$

the hyperbolic function in equation 24 allows asymptotic expansion

$$\chi_1 \approx \frac{2}{k_x h} \left(1 - \frac{k_x^2 h^2}{12} \alpha_{s1}^2 \right) = \frac{2}{k_x h} (1 + \beta), \quad (33)$$

where parameter

$$\beta = -i \frac{S^2}{12} \quad (34)$$

is expressed through the normalized skin factor,

$$S = h \sqrt{\frac{\omega \rho_f}{\eta}}. \quad (35)$$

For thin fractures, equation 30 yields

$$V_f^3 = V_{f0}^3 \frac{\beta}{1 + \beta}, \quad (36)$$

where V_{f0} is given by equation 1.

For $\beta \ll 1$, as follows from equation 36,

$$V_f = h \left(-i \frac{\omega^2 \mu_2}{12 \eta} (1 - \gamma^2) \right)^{\frac{1}{3}}. \quad (37)$$

For thick fractures, when

$$\left| \sqrt{1 - \alpha_{s1}^2} \frac{k_x h}{2} \right| \approx \frac{S}{2} \gg 1 \quad (38)$$

and $\chi_1 \approx -i\alpha_{s1}$, equation 30 gives the solution

$$V_f^3 = V_{f0}^3 \left(1 - \frac{1}{\sqrt{3}\beta} \right), \quad (39)$$

which approaches equation 1 of Ferrazzini and Aki (1987).

Equations 36 and 39 can be combined into a general form,

$$V_f^3 = V_{f0}^3 \frac{\beta}{1 + \sqrt{\beta/3} + \beta}, \quad (40)$$

where both asymptotics 32 and 33 are represented.

Biot slow wave

A fracture model with rigid walls (Figure 2) is also capable of carrying dispersive fluid waves with low velocity. In such a model, the interaction between walls and fluid occurs through viscous friction forces. For thin fractures, the fluid motion is directed mostly along the walls with a parabolic distribution across the fracture, which reaches the maximum at the centerline $z = 0$ and zero at the walls.

Introducing the total flow

$$F = \frac{1}{h} \int_{-\frac{h}{2}}^{\frac{h}{2}} u_x dz \quad (41)$$

across any $x = \text{constant}$ reduces equation 4 to

$$\frac{\partial^2 F}{\partial t^2} + \frac{12\eta}{h^2 \rho_f} \frac{\partial F}{\partial t} - \frac{\xi + \frac{4\eta}{3}}{\rho_f} \frac{\partial^2}{\partial x^2} \frac{\partial F}{\partial t} - c_p^2 \frac{\partial^2 F}{\partial x^2} = 0. \quad (42)$$

Note that fracture permeability $\kappa_{fr} = h^2/12$; therefore, it is embedded in the denominator of the second term of equation 42. In the frequency domain, equation 42 has the solution (Korneev et al., 2004)

$$F = \exp(i\tilde{k}x) \exp(-i\omega t), \quad \tilde{k} = k + i\alpha, \quad (43)$$

with the wavenumber k , the attenuation coefficient α , and the angular frequency ω . The wavenumber components have the forms

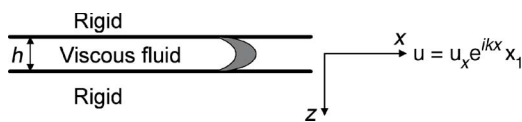


Figure 2. Biot's model for flow in fractures. Interaction of fluid with the fracture walls occurs because of the friction forces. Fluid moves predominantly along the rigid walls.

$$k = \frac{\omega}{c_p} \sqrt{\frac{\sqrt{(1+dg)^2 + (d+g)^2} + 1 + dg}{2(1+g^2)}}, \quad (44)$$

$$\alpha = \frac{\omega}{c_p} \sqrt{\frac{\sqrt{(1+dg)^2 + (d+g)^2} - 1 - dg}{2(1+g^2)}}, \quad (45)$$

where

$$d = \frac{12\eta}{\omega h^2 \rho_f} = \frac{\eta}{\omega \kappa_{fr} \rho_f}, \quad g = \frac{\omega \left(\xi + \frac{4\eta}{3} \right)}{\rho_f c_p^2}. \quad (46)$$

At low frequencies, the phase velocity V_f of the wave described by equation 43 has the asymptotic form

$$V_f = V_f^{\text{Biot}} = c_p \sqrt{\frac{\omega \kappa_{fr} \rho_f}{2\eta}} (1 - i), \quad (47)$$

similar to that for the slow Biot wave (Biot, 1956a, his equation 7.34). In fact, Biot uses the same model with rigid walls to describe the interaction of viscous fluid with rock pore walls (Biot, 1956b, 180). Thus, solutions 43–47 of equation 42 are the Biot-type solutions, in which the dispersive character of waves exists because of the finite viscosity of the fluid. At zero viscosity, both d and g in equations 46 vanish, and the wave given by equation 42 loses its frequency dependence. However, when the fracture-wall elasticity is taken into account, the existence of the slow fluid wave does not require a nonzero viscosity (equation 40).

The asymptotics of Biot's slow wave also can be obtained from equation 22 (B. Gurevich, personal communication, 2007) as another symmetrical mode. However, solutions 43–45 are preferred because of their explicit form in their entire frequency range.

NUMERICAL RESULTS

To estimate the possible effects of different fluids on the velocity and attenuation of the Stoneley guided wave, the computations are performed for two parameter cases: a 1-mm-thick fracture filled with water and oil of 0.01 and 0.05 poise viscosity, respectively. Five solutions are compared, the Biot solution (equations 43–46), the non-viscous fluid solution by Ferrazzini and Aki (equation 1), the exact solution for a viscous fluid, the general low-frequency asymptotic solution (equation 40), and its forms in equations 37 and 39. The exact solution for the viscous fluid is obtained by grid search for a complex root of equation 22. The results are shown in Figures 3 and 4. For the entire frequency range (1–1000 Hz), the left-hand side of inequality 28 does not exceed 5×10^{-3} , whereas the right-hand side of inequality 31 is larger than 10^4 .

DISCUSSION

For both fluids that were examined (water and oil), Biot's solution substantially overestimates the Stoneley-wave propagation velocities. This is predictable, because Biot's solution describes propagation of the body rather than surface waves. For water, the non-viscous-fluid solution gives a good approximation for the entire range of frequencies. For oil, it largely overestimates the velocities at low frequencies, where the differences between different fluids are most profound. The thin-fracture asymptotic (equation 36) quite accurately

ly predicts velocities at low frequencies, yielding only a constant-limit value for the Q factor. The general asymptotic (equation 40) describes reasonably well the exact solution at all frequencies. Surprisingly, the low velocities of Stoneley waves at seismic frequencies, which are in the range of tens of meters/second, result in wavelengths of about 3–10 m. Such wavelengths are comparable with the fracture lengths; therefore, the resonance conditions might be satisfied in finite fractures.

Indeed, let us consider a fracture with the length ℓ . Assuming the zero displacement condition $u(0) = 0$ at $x = 0$ and driving displacement $u(\ell) = u_0 \exp(-i\omega t)$ at $x = \ell$, we have the solution

$$u = u_0 A(\omega) \exp(-i\omega t),$$

$$A(\omega, x) = \frac{\exp\left(\frac{i\omega x}{V_f}\right) - \exp\left(\frac{-i\omega x}{V_f}\right)}{\exp\left(\frac{i\omega \ell}{V_f}\right) - \exp\left(\frac{-i\omega \ell}{V_f}\right)}, \quad (48)$$

where the phase velocity V_f is taken from equation 36. A numerical example, exhibiting resonant behavior of a slow fluid wave in a 4-m-

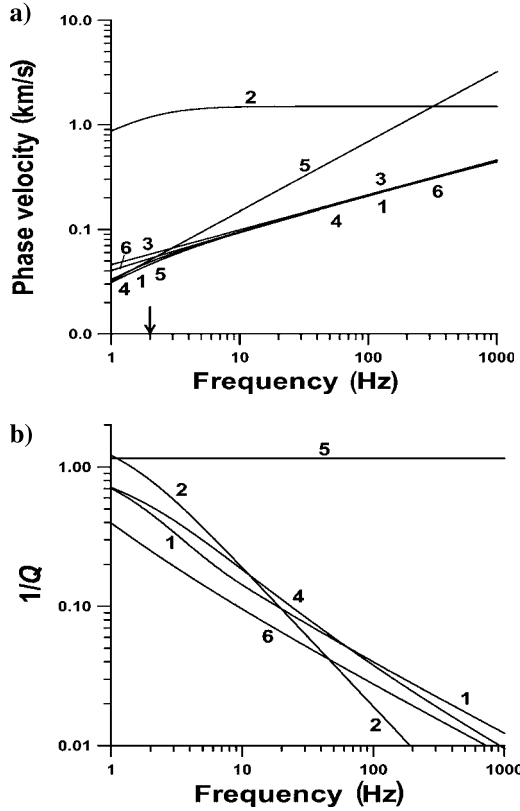


Figure 3. Comparison of solutions for a water-filled, 1-mm-thick fracture as functions of frequency. The curves are marked as follows: (1) exact solution for a viscous fluid in an elastic fracture computed via roots of equation 22; (2) Biot's solution from equations 43–45; (3) solution for nonviscous fluid given by equation 1; (4) general asymptotic (equation 40); (5) thin-fracture asymptotic (equation 37); (6) thick-fracture asymptotic (equation 39). (a) Phase velocities. (b) Inverse of quality factor Q . Note that the propagation velocities are small. All fluid-elastic solutions have about the same velocity dependencies, but the differences in attenuation are quite large. The values of Q at seismic frequencies reach 20. Vertical arrow indicates frequency for $S = 1$.

long fracture, is shown in Figure 5 for water infill and in Figure 6 for oil infill of a fracture with 1-mm thickness. In those figures, the amplitude-square average

$$E(\omega) = \frac{1}{\ell} \int_0^\ell |A(\omega, x)|^2 dx \quad (49)$$

is shown. The first resonant peak occurs at 14 Hz for water and at 12 Hz for oil. Predictably, the peaks for the water-filled fractures are sharper and higher than those for the oil-filled fractures.

After applying equation 1 for phase velocity in thick fractures and using solution 48, the resonant frequencies can be estimated from the following formula:

$$\omega_k = (1 + 2k) \sqrt{\frac{\pi^3 h \mu}{\ell^3 \rho_f} (1 - \gamma^2)}, \quad k = 0, 1, 2, \dots \quad (50)$$

For $k = 0$, equation 50 evaluates the first resonance frequency as equal to 13.8 Hz, a good approximation for the exact resonant frequency. For a thin fracture, equation 37 can be applied, and the amplitude-square average (equation 49) has the form

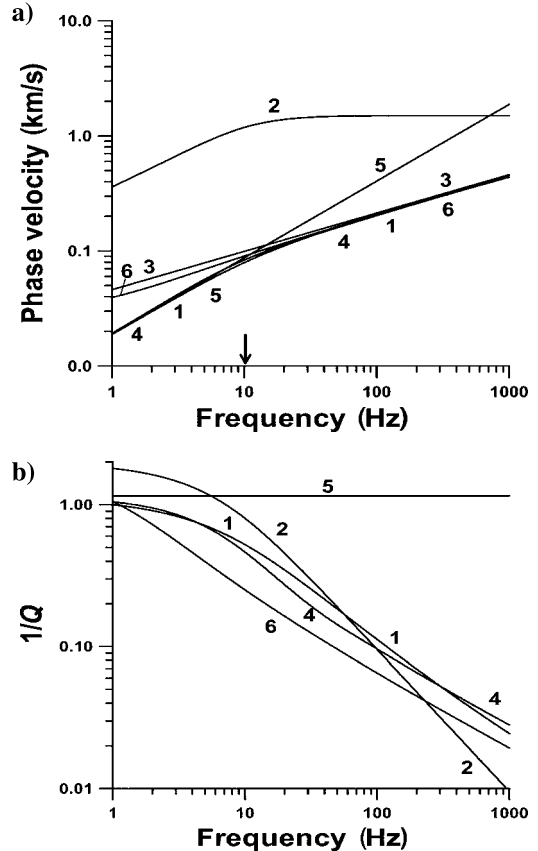


Figure 4. Same as in Figure 3 but for oil-filled fractures. The small S asymptotic provides a good approximation for the exact solution, which differs significantly from the nonviscous fluid solution. The values of Q at seismic frequencies reaches 10. The main differences between water-filled (Figure 3) and oil-filled fractures are observed at low frequencies. (a) Phase velocities. (b) Inverse of quality factor Q .

$$E(\omega) = \frac{1 - \exp(-2w)}{w}, \quad (51)$$

where

$$w = \frac{\ell}{h} \left(\frac{12\omega\eta}{\mu_2(1 - \gamma^2)} \right)^{\frac{1}{3}}. \quad (52)$$

Figure 7 compares the exact solution and approximation 51 for an oil-filled fracture with 0.1-mm thickness. Both exhibit an increase in amplitude response as the frequency approaches zero. This interesting behavior, as well as the velocity differences for water and oil infills (Figures 3 and 4), might be parts of mechanisms responsible for yet unexplained low-frequency signatures observed for hydrocarbon reservoirs (Castagna et al., 2003; Korneev et al., 2004; Goloshubin et al., 2006).

Thus, the solution for the Stoneley slow waves generated in a viscous fluid indicates that, even for a rather thin fracture, Q can be large enough to allow the fluid-wave resonances. Considering the statistical distribution of fracture sizes, we might expect that at any given frequency, resonant conditions will be satisfied for some fracture population. Then it would be natural to expect a strong interac-

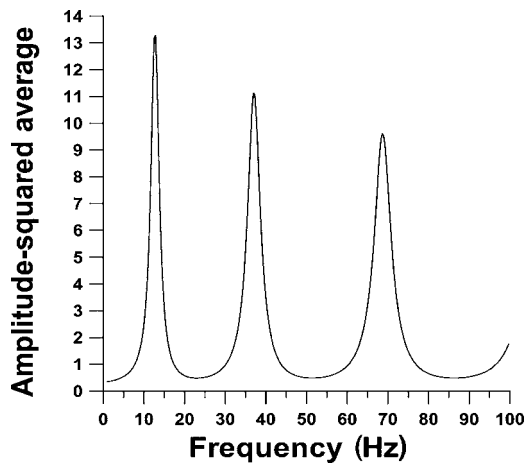


Figure 5. Resonant energy density for a 4-m-long, 1-mm-thick water-filled fracture.

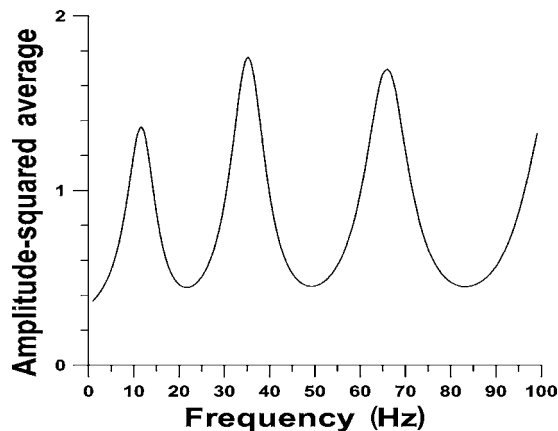


Figure 6. Same as in Figure 5 but for an oil-filled fracture.

tion of slow waves in systems of intersecting fluid-filled fractures.

The fluid-filled fractures represent strong waveguides with relatively large wave amplitudes. A qualitative estimate of an amplitude A_f for a wave propagating with velocity V_f in a medium with density ρ_f compared to an incident wave with amplitude A_o in a medium with parameters V_o and ρ_o has the approximate form

$$\frac{A_f}{A_o} = \sqrt{\frac{V_o\rho_o}{V_f\rho_f}}. \quad (53)$$

Using the values $V_o = 4000$ m/s and $\rho_o = 2.7$ g/cm³ for the incident P-wave and $V_f = 20$ m/s and $\rho_f = 1$ g/cm³ for the Stoneley guided wave, we get a 25-fold increase in the fluid-wave amplitude. Note that this estimate is consistent with the numerical results of Groenenboom and Falk (2000). Furthermore, at resonances, the amplitude rise is approximately equal to Q , and we might have an extra tenfold amplitude increase (Figure 3).

Fractures play a major role in determining the permeability and direction of fluid flow in rocks at field scales. This is especially true for oil reservoirs. In most rocks and at all scales, fractures generally have a hierarchical self-similar distribution. Fluid-filled fractures provide sharp velocity contrasts with dispersive Stoneley fluid waves and are likely to be capable of strongly absorbing energy from passing seismic waves. The energy absorption can increase tenfold when the resonant conditions are met, which might create favorable conditions for nonlinear fluid-flow effects. The resonant conditions for fracture-fluid waves can exist even below typical seismic frequencies when the slow-wave velocities approach zero. Fracture systems also represent contrast scattering media for propagating seismic waves.

All of the above phenomena should lead to strongly frequency-dependent propagation effects for seismic waves, which affect both velocity and attenuation. Existing poroelastic theories that consider fractures in their models (Barenblatt et al., 1960; Mavko and Nur, 1975; Dvorkin and Nur, 1993; Dvorkin et al., 1994; Pride and Berryman, 2003a, b) treat fractures just as channels for viscous fluid flow, similar to Biot's model and without incorporating physics for the Stoneley slow waves. It might be possible that such incorporation is critically important for wave-propagation effects in fractured reservoirs. Several studies describe the elastic properties of materials

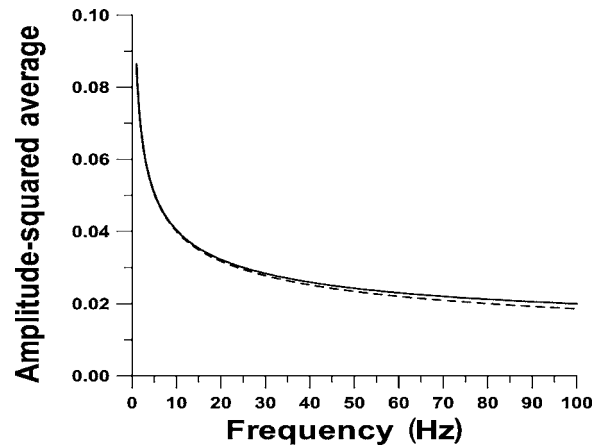


Figure 7. Amplitude-squared average for a thin fracture filled with oil. Exact solution (solid line) is compared with the analytical approximation given by equation 51 (dashed line). Low frequencies yield higher-amplitude responses.

containing fluid-saturated noninteracting fractures (O'Connell and Budiansky, 1977; Garbin and Knopoff, 1975; Hudson, 1980, 1981). It remains unclear whether the Stoneley slow wave survives in asymptotic solutions for small fractures. Careful numerical modeling of interaction between propagating body waves and fluid-filled fractures is needed to address those problems. However, such modeling presents a major computational challenge because of the coexistence of wavelengths that have dramatically different sizes.

An adequate theory that can be applied at field scales needs to incorporate fluid-elastic interactions in fractures and self-similar fracture distribution. For proper extraction of permeability information, the scattering of seismic waves caused by fracturing within such heterogeneous systems needs to be taken into account.

It is yet unclear how well the idealized fracture models used in this study represent fractures in real rocks that have complex surface topography and varying thicknesses. One can speculate that the details of fracture geometry are not very important at low frequencies. This problem is being studied in a series of laboratory measurements.

CONCLUSIONS

The analytical solution has been obtained for the phase velocity of the Stoneley guided wave for an infinite fracture filled with a viscous fluid. The solution suggests the possibility of differentiating between oil and water at low frequencies. It also suggests that resonances at seismic frequencies are possible at the reservoir scale. The Stoneley-wave (slow-wave) effect, which is not a part of any existing poroelastic theory, needs to be taken into account at field scales.

ACKNOWLEDGMENTS

This work was supported by the National Energy Technology Laboratory, Office of Fossil Energy Sciences, of the U. S. Department of Energy under contract DE-AC03-76SF00098. The author thanks Jim Berryman, Dmitry Silin, and Michael Schoenberg for helpful comments. The paper was improved greatly from discussions with Boris Gurevich.

REFERENCES

- Barenblatt, G. I., I. P. Zheltov, and I. N. Kochina, 1960, Basic concepts in the theory of seepage of homogeneous liquids in fissured rocks: *Journal of Applied Mathematics*, **24**, 1286–1303.
- Biot, M. A., 1956a, Theory of propagation of elastic waves in a fluid-saturated porous solid — I: Low-frequency range: *Journal of the Acoustical Society of America*, **28**, 168–178.
- , 1956b, Theory of propagation of elastic waves in a fluid-saturated porous solid — II: Higher frequency range: *Journal of the Acoustical Society of America*, **28**, 179–191.
- , 1962, Mechanics of deformation and acoustic propagation in porous media: *Journal of Applied Physics*, **33**, 1482–1498.
- Castagna, J. P., S. Sun, and S. R. Wu., 2003, Instantaneous spectral analysis: Detection of low-frequency shadows associated with hydrocarbons: *The Leading Edge*, **22**, 120–127.
- Chouet, B., 1986, Dynamics of a fluid-driven crack in three dimensions by the finite-difference method: *Journal of Geophysical Research*, **91**, 13967–13992.
- Clauser, C., 1992, Permeability of crystalline rocks: *EOS Transactions of the American Geophysical Union*, **73**, no. 21, 233.
- Dvorkin, J., R. Nolen-Noeksema, and A. Nur, 1994, The squirt-flow mechanisms: Macroscopic description: *Geophysics*, **59**, 428–438.
- Dvorkin, J., and A. Nur, 1993, Dynamic poroelasticity: A unified model with the squirt and Biot mechanisms: *Geophysics*, **58**, 524–533.
- Ferrazzini, V., and K. Aki, 1987, Slow waves trapped in a fluid-filled infinite crack: Implications for volcanic tremor: *Journal of Geophysical Research*, **92**, 9215–9223.
- Garbin, H. D., and L. Knopoff, 1975, Elastic moduli of a medium with liquid-filled cracks: *Quarterly of Applied Mathematics*, **32**, 301–303.
- Gassmann, F., 1951, Über die elastizität poroser Medien: *Vierteljahrsschrift der Naturforschenden Gesellschaft in Zurich*, **96**, 1–23.
- Gelhar, L. W., 1993, *Stochastic subsurface hydrology*: Prentice-Hall, Inc.
- Goloshubin, G. M., V. A. Korneev, D. B. Silin, V. S. Vingalov, and C. Vanshuyer, 2006, Reservoir imaging using low frequencies of seismic reflections: *The Leading Edge*, **25**, 527–531.
- Goloshubin, G. M., P. V. Krauklis, L. A. Molotkov, and H. B. Helle, 1994, Slow wave phenomenon at seismic frequencies: 63rd Annual International Meeting, SEG, Expanded Abstracts, 809–811.
- Groenenboom, J., and J. Falk, 2000, Scattering by hydraulic fractures: Finite-difference modeling and laboratory data: *Geophysics*, **65**, 612–622.
- Groenenboom, J., and J. T. Fokkema, 1998, Guided waves along hydraulic fractures: 67th Annual International Meeting, SEG, Expanded Abstracts, 139–148.
- Groenenboom, J., and D. B. van Dam, 2000, Monitoring hydraulic fracture growth: Laboratory experiments: *Geophysics*, **65**, 603–611.
- Gurevich, B., 2002, Effect of fluid viscosity on elastic wave attenuation in porous rocks: *Geophysics*, **67**, 264–270.
- Hornby, B. E., D. L. Johnson, K. W. Winkler, and R. A. Plumb, 1989, Fracture evaluation using reflected Stoneley-wave arrivals: *Geophysics*, **54**, 1274–1288.
- Hudson, J. A., 1980, Overall properties of a cracked solid: *Mathematical Proceedings of the Cambridge Philosophical Society*, **99**, 371–384.
- , 1981, Wave speeds and attenuation of elastic waves in material containing cracks: *Geophysical Journal of the Royal Astronomical Society*, **64**, 133–150.
- Korneev, V. A., G. M. Goloshubin, T. V. Daley, and D. B. Silin, 2004, Seismic low-frequency effects in monitoring of fluid-saturated reservoirs: *Geophysics*, **69**, 522–532.
- Kostek, S., D. L. Johnson, and C. J. Randall, 1998a, The interaction of tube waves with borehole fractures, part I: Numerical models: *Geophysics*, **63**, 800–808.
- Kostek, S., D. L. Johnson, K. W. Winkler, and B. E. Hornby, 1998b, The interaction of tube waves with borehole fractures, part II: Analytical models: *Geophysics*, **63**, 809–815.
- Krauklis, P. V., 1962, About some low frequency oscillations of a liquid layer in elastic medium (in Russian): *Prikladnaya Matematika i Mekhanika (Journal of Applied Mathematics and Mechanics)*, **26**, 1111–1115.
- Landau, L. D., and E. M. Lifshitz, 1959, *Fluid mechanics*: Pergamon Press, Inc.
- Mavko, G., and A. Nur, 1975, Melt squirt in asthenosphere: *Journal of Geophysical Research*, **80**, 1444–1448.
- Molotkov, L. A., and A. V. Bakulin, 1998, The effective model of a stratified solid-fluid medium as a special case of the Biot model: *Journal of Mathematical Sciences*, **91**, 2812–2826.
- Muskat, M., 1946, *The flow of homogeneous fluids through porous media*: J. W. Edwards, Inc.
- Neuman, S. P., 1994, Generalized scaling of permeabilities: Validation and effect of support scale: *Geophysical Research Letters*, **21**, 349–352.
- O'Connell, R. J., and B. Budiansky, 1977, Viscoelastic properties of fluid saturated cracked solids: *Journal of Geophysical Research*, **82**, 5719–5735.
- Paillet, F. L., and J. E. White, 1982, Acoustic models of propagation in the borehole and their relationship to rock properties: *Geophysics*, **47**, 1215–1228.
- Pride, S. R., and J. G. Berryman, 2003a, Linear dynamics of double-porosity dual-permeability materials — I: Governing equations and acoustic attenuation: *Physical Review E*, **68**, 036603.
- , 2003b, Linear dynamics of double-porosity dual-permeability materials — II: Fluid transport equations: *Physical Review E*, **68**, 036604.
- Schoenberg, M. A., 1983, Wave propagation in a finely laminated periodic elastoacoustic medium: *Applied Physics Letters*, **42**, no. 4, 350–352.
- , 1984, Wave propagation in alternating solid and fluid layers: *Wave Motion*, **6**, no. 3, 303–320.
- Schulze-Makuch, D., D. A. Carlson, D. S. Cherkauer, and P. Malik, 1999, Scale dependency of hydraulic conductivity in heterogeneous media: *Ground Water*, **37**, 904–919.
- Schulze-Makuch, D., and D. S. Cherkauer, 1998, Variations in hydraulic conductivity with scale of measurements during aquifer tests in heterogeneous, porous carbonate rock: *Hydrogeology Journal*, **6**, 204–215.